

NASA
TP
1816
c. 1

NASA Technical Paper 1816

Stochastic Analysis of Spectral Broadening by a Free Turbulent Shear Layer

Jay C. Hardin and John S. Preisser

MAY 1981

LOAN COPY:
AFWL TECHN
KIRTLAND AF

0134958



TECH LIBRARY KAFB, NM

NASA



NASA Technical Paper 1816

Stochastic Analysis of Spectral Broadening by a Free Turbulent Shear Layer

Jay C. Hardin and John S. Preisser
Langley Research Center
Hampton, Virginia



National Aeronautics
and Space Administration

**Scientific and Technical
Information Branch**

1981

INTRODUCTION

For many years, it has been recognized that sound propagating through a medium whose properties are variable may be altered in character (ref. 1). In particular, the direction of propagation of the sound and the intensity of sound received by an observer depend dramatically on the physical properties of the intervening medium. Various aspects of this phenomenon have been studied by numerous researchers. For example, Ribner (ref. 2) solved by Fourier analysis for the refraction of a plane sound wave by a shear layer of zero thickness. Candel et al. (ref. 3) considered the propagation of an acoustic field in a free jet by using a high frequency geometric approximation. Howe (ref. 4) evaluated multiple scattering of sound by frozen turbulent eddies. Much of this work has been reviewed by Lighthill (ref. 5).

Recently, this problem has again begun to receive attention because of the increased use of open jet flow facilities for testing aeroacoustic sources. Of interest are the effects of the shear layer between the free jet and the surrounding ambient medium on the measured intensity, directivity, and spectra of the noise source when compared to those which would be measured if the source were in flight. Studies primarily of the required angle and amplitude corrections have been accomplished by Schlinker and Amiet (ref. 6), Ahuja et al. (ref. 7), and Ozkul and Yu (ref. 8).

Although these direction and intensity changes are the dominant effects of propagation through a shear layer, a significant frequency distortion has been observed as well (ref. 9). This phenomenon is the spectral broadening which becomes apparent when a tonal or narrow-band source is present in the jet. Sound power which is radiated at a given frequency is perceived outside the jet as a band of frequencies scattered about the original frequency.

In a recent paper, Schlinker and Amiet (ref. 9) have speculated that this "frequency scattering" may be caused by a Doppler shift produced as the sound traverses convecting turbulent eddies in the flow as if the sound were absorbed by the eddy and then reemitted from the eddy as a moving source. Superposition of this Doppler-shifted sound with the "remnant" of the original sound wave which did not encounter an eddy during its passage would then produce a frequency shift at the observer location, as well as a low frequency modulation of the acoustic signal.

Although such a model can account for the observed phenomenon, it is unnecessary to require an actual Doppler shift in the frequency. An alternate model can be developed by supposing that a sound wave would merely traverse an eddy, being somewhat distorted in amplitude and phase by its passage. In this case, there would be no Doppler shift. Such phenomena have previously been described in the classic works by the Russian workers, Chernov (ref. 10) and Tatarski (ref. 11), who were primarily interested in propagation of radio waves through a turbulent atmosphere. The possibility of spectral broadening in this case is well documented in electromagnetic theory (ref. 12).

In the present paper, we show that the apparent frequency shift observed in the spectral data can be explained purely on the basis of amplitude modulation by the time variation of the shear layer between the source and observer. This theory is then supported by experimental data obtained at Langley Research Center in which no frequency shift can be observed, although modulation is obvious.

ANALYSIS

Consider the geometry shown in figure 1. A source of frequency ω_0 lies immersed in a flow with axial velocity U_0 . (The symbols used in this analysis

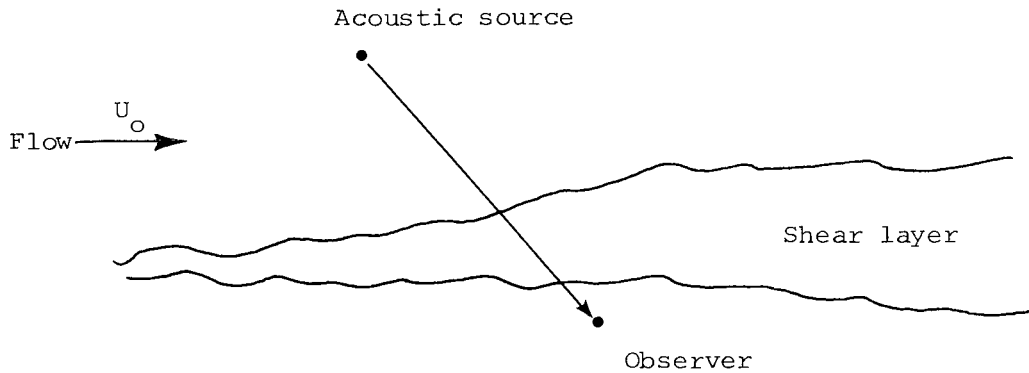


Figure 1.- Geometry of free-jet acoustic test.

are defined at the back of this paper on p. 23.) Between the source and an observer situated outside the flow in an ambient region lies a shear layer through which the axial velocity drops from U_0 to zero. This shear layer is, in general, turbulent and thus presents a time-varying medium through which the sound must propagate to the observer. The question of interest is the effect of this shear layer on the observed frequency of the sound radiation.

The nonturbulent theory of sound propagation for this geometry (see ref. 9 for an extensive review) would yield no frequency shift, since there is no relative motion between the source and observer. Thus, if the time dependence of the shear layer is neglected, the acoustic pressure signal reaching the observer would be

$$p(t) = A_0 \cos (\omega_0 t + \phi)$$

where the amplitude A_0 is a constant dependent on the intensity and directivity of the source, the velocity of the flow, and the distance from the source to the observer; and the phase angle ϕ is a random variable uniformly distributed over $(0, 2\pi)$ dependent on the choice for the origin of time t . In this

case, the expected value of the acoustic pressure can be shown to be zero, and its autocorrelation depends only on the time difference τ , i.e.,

$$R_{pp}(\tau) = E[p(t) p(t+\tau)] = \frac{A_0^2}{2} \cos \omega_0 \tau \quad (1)$$

where $E[]$ is the expectation operator. Thus, the acoustic pressure is a weakly stationary random process (ref. 13) whose power spectral density consists of two delta functions:

$$S_p(\omega) = \frac{A_0^2}{4} [\delta(\omega - \omega_0) + \delta(\omega + \omega_0)] \quad (2)$$

as shown in figure 2. For future reference, note that the power of the acoustic signal at the observer is

$$E[p^2(t)] = R_{pp}(0) = \frac{A_0^2}{2} \quad (3)$$

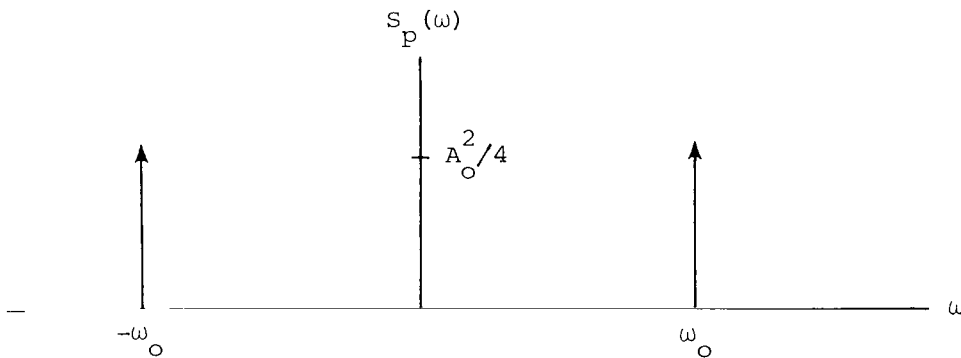


Figure 2.- Power spectral density of observer signal for time-independent flow.

Consider now the effect of the time dependence of the flow on sound radiation from this source. It is assumed only that the source impedance is such that the time dependence of the flow does not alter the fundamental frequency at which the source radiates and that the acoustic pressure received by the observer is at least a weakly stationary random process. The latter assumption is, of course, generally made in the analysis of such data and is an entirely reasonable expectation for such geometry.

If the time-dependent shear layer produces an amplitude modulation of the acoustic signal, the acoustic pressure at the observer may then be written

$$p(t) = A(t) \cos (\omega_0 t + \phi)$$

where $A(t)$, a random process independent of the random variable ϕ , represents the modulating effect of the shear layer on the amplitude of the acoustic wave. This is a classic random process which many have studied (see, for example, Papoulis (ref. 13)). Since Schlinker and Amiet (ref. 9) have shown that the effects of the time variation of the shear layer are small, one should expect that

$$E[A(t)] = A_0$$

The expected value of the amplitude-modulated acoustic signal remains zero, and its autocorrelation is given by

$$R_{AM}(\tau) = E[p(t) p(t+\tau)] = \frac{E[A(t) A(t+\tau)]}{2} \cos \omega_0 \tau \quad (4)$$

Thus, for the acoustic signal to be weakly stationary, it is necessary and sufficient for the autocorrelation of the amplitude modulation to depend only upon the time difference, i.e.,

$$R_A(\tau) = E[A(t) A(t+\tau)]$$

Then,

$$R_{AM}(\tau) = \frac{R_A(\tau)}{2} \cos \omega_0 \tau \quad (5)$$

where it can be seen that the autocorrelation of the amplitude-modulated acoustic wave is merely a product of the correlation coefficient of the undistorted wave with the autocorrelation of the amplitude modulation.

Note also that the power in the acoustic signal is now

$$E[p^2(t)] = R_{AM}(0) = \frac{R_A(0)}{2} \quad (6)$$

If the amplitude modulation does not change the mean amplitude, that is, if we can write $A(t) = A_0 + \epsilon(t)$ where $E[\epsilon(t)] = 0$, then

$$R_A(0) = E[A^2(t)] = A_0^2 + E[\epsilon^2(t)] \geq A_0^2$$

Thus, by comparing equations (3) and (6), it can be seen that amplitude modulation which does not change the mean amplitude must always increase the power of the acoustic signal over that of the unmodulated signal. Such amplification of an acoustic signal by passage through a shear layer has been observed by Maestrello et al. (ref. 14). The autocorrelation of the modulating process may then be written

$$R_A(\tau) = A_0^2 + R_\epsilon(\tau)$$

which has the behavior shown in figure 3, since $R_\epsilon(\tau)$ approaches $E^2[\epsilon(t)] = 0$ as $\tau \rightarrow \infty$.

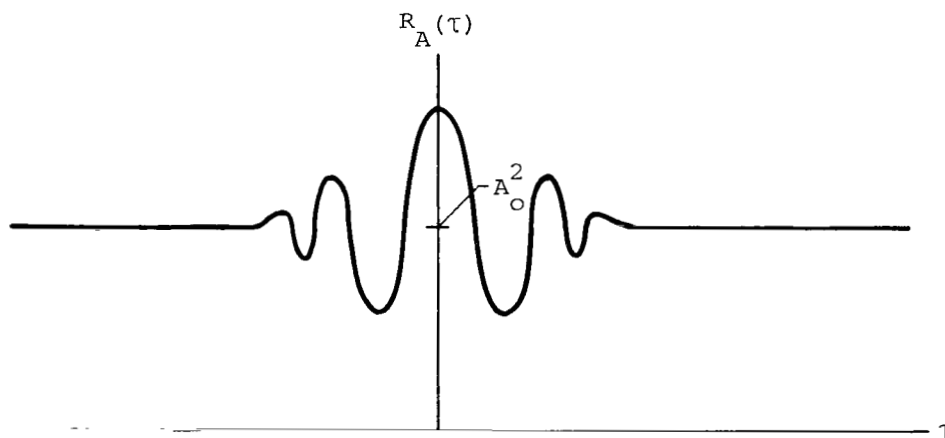


Figure 3.- Autocorrelation of amplitude-modulation process.

By introducing the power spectral density of the amplitude-modulation process,

$$S_A(\omega) = \frac{1}{2\pi} \int_{-\infty}^{\infty} R_A(\tau) e^{-i\omega\tau} d\tau$$

it can then be shown by noting equation (5) that the power spectral density of the amplitude-modulated acoustic signal is just

$$S_{AM}(\omega) = \frac{1}{4} [S_A(\omega - \omega_0) + S_A(\omega + \omega_0)]$$

which is the typical spectrum for a narrow-band random process (ref. 13). The characteristics of this spectrum may be visualized by observing that the frequencies of the shear layer are usually low compared with typical source frequencies (the characteristic frequency of the shear layer is of the order of U_0/l , where l is the thickness of the layer). Thus, the power of the amplitude-modulation process is clustered about the frequency of zero, with a delta function at $\omega = 0$ due to the large nonzero lag of the autocorrelation, and the spectral density of the amplitude-modulated acoustic signal appears as shown in figure 4. Thus, amplitude modulation can produce the observed broadening in the frequency domain as well as the "remnant" of the original discrete tone noted by Schlinker and Amiet (ref. 9).

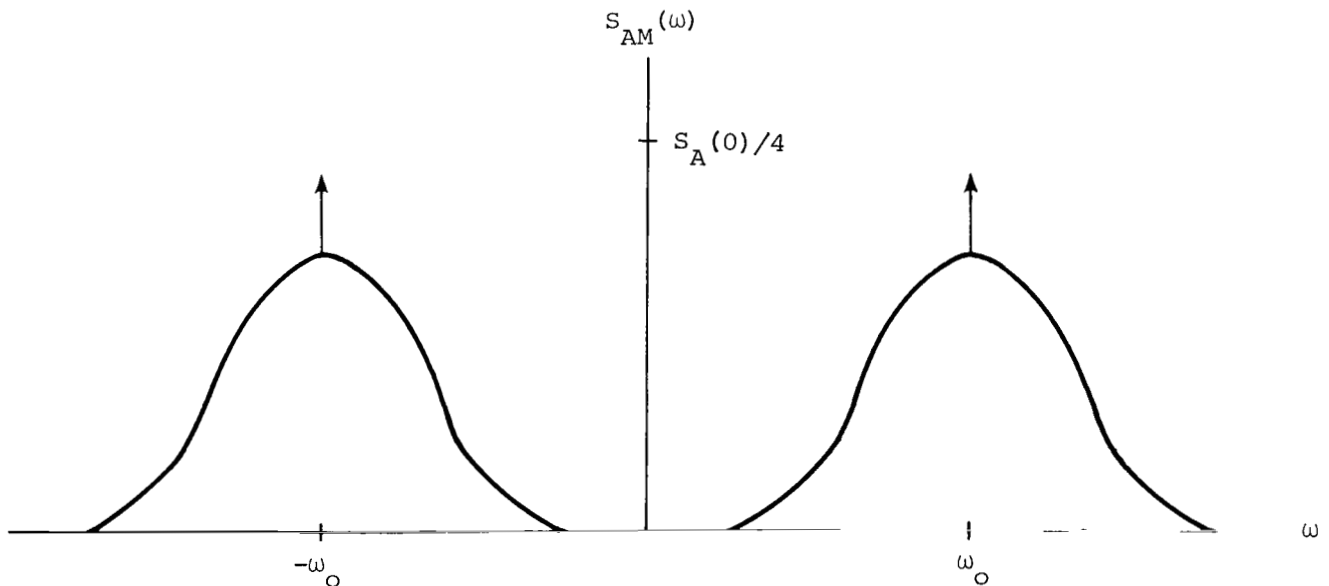


Figure 4.- Power spectral density of amplitude-modulated acoustic pressure.

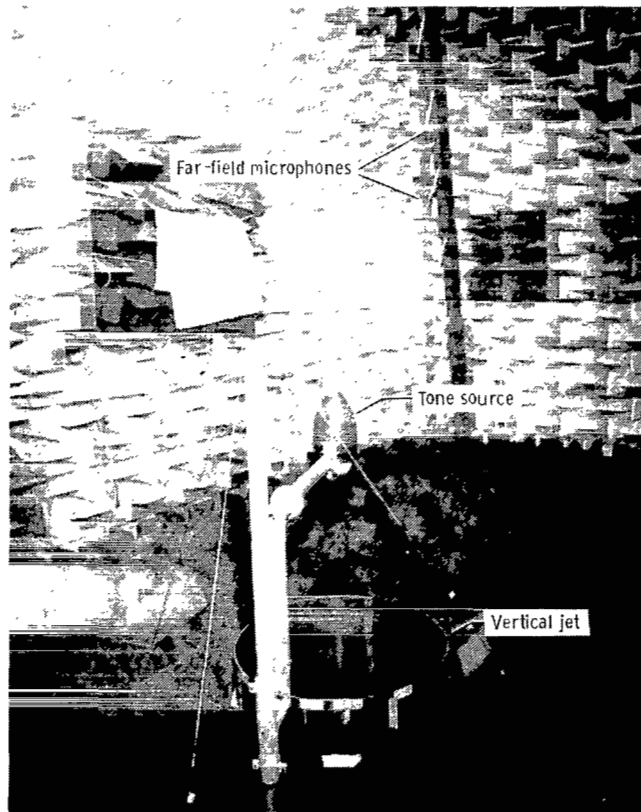
Some readers may be interested in comparing this theory with the effect of a pure frequency modulation. This comparison is made in the appendix where it is shown that frequency modulation can produce an acoustic pressure autocorrelation, and thus power spectral density, similar to that produced by amplitude modulation. Thus, there may be no differentiation between the two on a spectral basis, and only by observing the time histories can such a characterization be attempted.

In the next section, experimental data obtained at Langley Research Center for an acoustic source in free jet flow are presented. The time histories produced by this experiment display obvious amplitude modulation, but no apparent frequency shift. These data are then analyzed to estimate certain properties of the amplitude-modulation process described above.

DESCRIPTION OF EXPERIMENT

Experimental Setup

The test was performed at the Langley Aircraft Noise Reduction Laboratory in the Langley Anechoic Noise Facility. Figure 5 shows a photograph of the tone



L-80-535.1

Figure 5.- Photograph of source in Langley Anechoic Noise Facility.

source mounted in the anechoic room. Figure 6 presents dimensions pertinent to the setup. The room is 6.1 m wide, 9.2 m long, and 7.1 m high and has 0.84-m-deep fiberglass wedges on the floor, walls, and ceiling. The tone source was sting mounted 1.52 m above the exit plane of a vertical jet. The jet, 1.22 m in diameter, was driven by a centrifugal fan that is housed in another building.

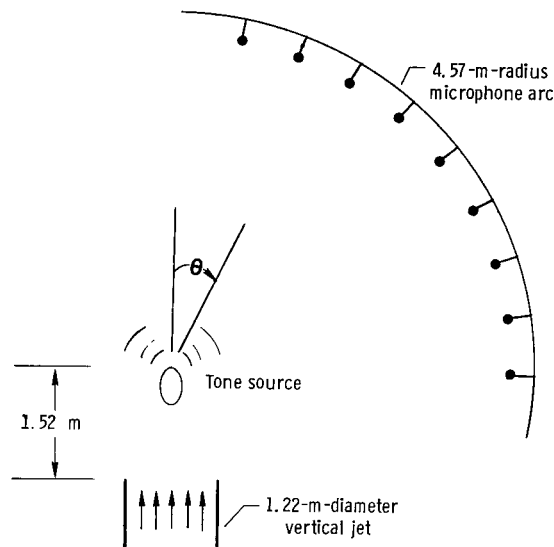


Figure 6.- Schematic of experimental setup.

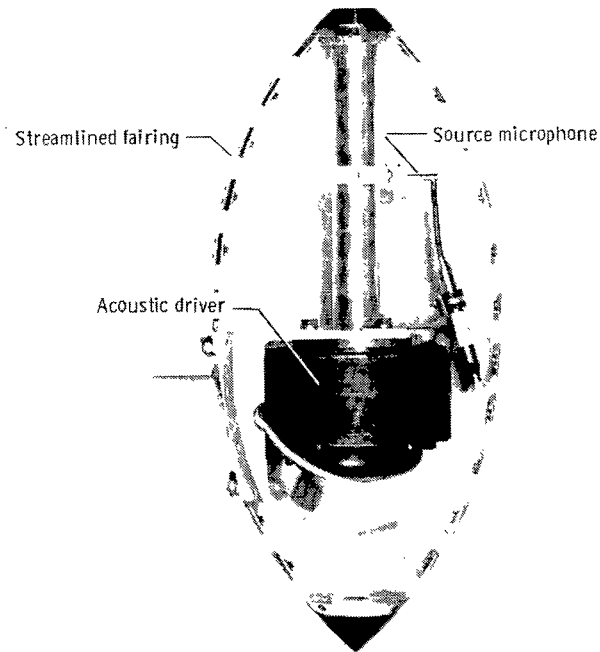
The air passes through several muffler sections on its way to the anechoic room. This design feature minimizes extraneous background noise entering the facility.

One-half-inch condenser-type free-field microphones fitted with sharp noise cones to reduce unwanted wind noise were secured to a rigid arc that extended from the floor to the ceiling. The arc was covered with sections of fiberglass wedges to minimize reflections of the acoustic signal. The microphones were placed at a constant radius of 4.57 m from the source in 10° angular increments from 10° to 90° . Except for the top two, which experienced intermittent buffeting by the jet flow, the microphones were outside the flow field.

A cutaway view of the tone source is presented in figure 7. The source was originally designed to be flown under the wing of an aircraft. As such, it consisted of a high intensity acoustic driver coupled to a long cylindrical tube and encased in a streamlined fairing. The tube was 30.5 cm long and had a 3.5-cm inner diameter to match the size of the diaphragm of the driver. This arrangement generated plane waves at the driver frequency. A one-eighth-inch microphone was flush mounted in the wall of the tube to monitor the source strength. The end of the tube was covered with a single layer of fiberglass cloth to inhibit unsteady aerodynamic fluctuations which affect the acoustic source and to keep the driver and source microphones clean. The cloth is known to have between 80 and 90 percent transmissibility. Any change in the impedance at the cloth location due to flow would change the standing wave pattern inside the tube. The source microphone was closely monitored at all times to ensure no change in the standing wave pattern, and consequently no change in the radiation efficiency occurred.

Flow Field

Unpublished hot-wire and pitot tube surveys of the 1.22-m-diameter vertical jet indicated that the jet spread much like a classical subsonic jet with the



L-79-7363.1

Figure 7.- Cutaway view of acoustic source.

potential core extending approximately five diameters downstream. In addition, the normalized mean velocity profile shape for a given downstream station was independent of the value of centerline velocity and uniform to within 1 or 2 percent. Typical profiles are presented in figure 8. The acoustic source

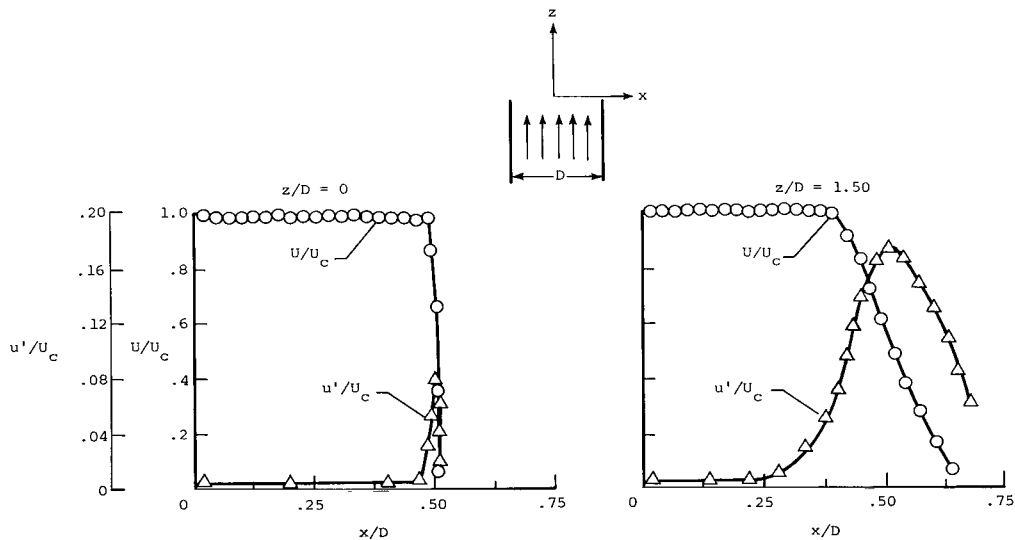


Figure 8.- Mean and turbulent velocity profiles at two downstream locations.

was not in place when these measurements were made. Profiles of both mean jet velocity U and root-mean-square turbulent velocity u' are shown normalized by the centerline velocity U_c . One profile presented is for a downstream position ($z/D = 1.50$) not far from the tone source. The data show the growth of the shear layer width and the increase in turbulent intensity from the exit plane ($z/D = 0$) to the downstream location. Near the tone source, the turbulent levels in the core were on the order of 0.5 percent, while in the shear layer, levels peaked at 18 percent.

Note that with the source in place, there would be an increase in the turbulence level near the jet centerline caused by the wake of the source itself. The intensity and lateral extent of the turbulent wake, however, would be small compared with the jet shear layer. Moreover, the analysis presented previously in this paper is independent of the position of the turbulent region through which the tone traverses. Hence, the results should not be affected by the source wake.

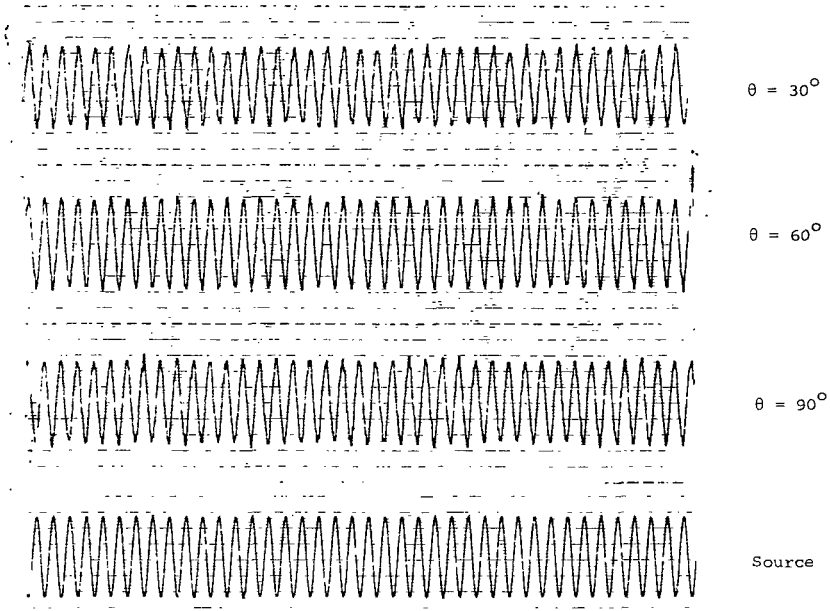
Procedure

Tests were conducted at tone frequencies of 2, 4, and 6 kHz and at jet velocities of 10, 20, and 30 m/s. Data from the nine far-field microphones and source microphone were high-pass filtered at 1000 Hz and recorded on magnetic tape for post-test data analysis. Power spectra are presented herein from the 30° , 60° , and 90° microphones and were obtained with the aid of a spectral analyzer using a bandwidth of analysis of 12.5 Hz. Normalized autocorrelations of data were calculated using results from a general time series analysis program. These calculations are discussed further in a later portion of this report.

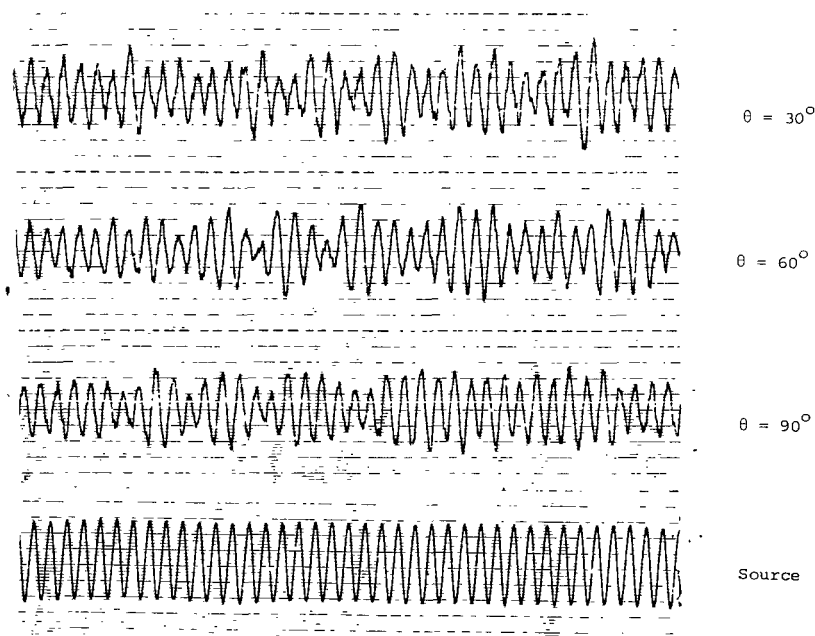
DATA PRESENTATIONS

Time Histories

Figure 9 presents sample time histories of the pressure signals for both the source and the far-field microphone. The data represent 20-ms bursts at a source frequency of 2 kHz. Figure 9(a) presents results for no jet flow; figure 9(b) corresponds to a jet velocity of 30 m/s. For both cases, the source appears as a nearly perfect sinusoidal function. The jet flow changed the root-mean-square pressure by less than 0.25 dB. On the other hand, the far-field microphones show considerable change, due to propagation of the tone through the shear layer of the jet. Note that the instantaneous amplitude of the tone in the far field has undergone considerable change, although there is no readily discernible frequency change. This result provides solid support to the choice of amplitude modulation as the cause of the spectral broadening observed in the frequency domain. Additional analysis to follow affirms this conclusion.



(a) No flow.



(b) 30-m/s jet velocity.

Figure 9.- Microphone time histories. 20-ms record length; 2-kHz signal.

Narrow-band Spectra

Figure 10 presents narrow-band power spectra (12.5-Hz bandwidth) for the 30° far-field microphone at several jet velocities. This particular angle was chosen so that the tone would traverse a relatively thick part of the shear layer. The source was radiating at 4 kHz. With no jet velocity, the spectra show a 83-dB spike at the source frequency. The first harmonic is evident about 31 dB lower. As jet velocity increases, the figure shows a gradual decrease in the tone amplitude and a simultaneous broadening of the spectra. In addition, broadband flow noise increases with increasing velocity. Measurements taken with the source off and jet on indicate no change in the jet noise spectra due to the source. The decrease in tone amplitude suggested the occurrence of direction scattering of sound to new angles, and the broadening effect was attributed to Doppler-shifting by the authors of reference 9. In a subsequent section of the paper, an alternate explanation is presented.

Figure 11 presents the effects of far-field angle θ on the scattered tone. The data show that the broadening effect occurs at all angles with the largest effect occurring at 30°. Changes in tone amplitude with angle are not meaningful in figure 11, since the source directivity was not uniform in θ , but slowly decreased with increasing angle.

Figure 12 presents the effects of tone frequency on scattering. Again, changes in tone amplitude cannot be compared directly, since the radiation efficiency of the source changes with frequency. There appears to be more broadening at the higher frequencies; however, the effect does not appear to be significant. It was found in reference 9 that scattering becomes most significant as the ratio of shear layer propagation path to the acoustic wavelength becomes larger than 10. For the present data with shear layer thicknesses estimated from figure 8, this ratio was less than 5. Hence, any frequency effect would be difficult to extract from the experimental data.

DATA ANALYSIS

In this section, the data presented previously are analyzed in an attempt to emphasize the amplitude-modulation effect of the time-varying shear layer. Note from equation (5) that the role of the shear layer in the theoretical analysis can be extracted by dividing the autocorrelation of the acoustic signal by $\cos \omega_0 \tau$, i.e.,

$$\frac{R_{AM}(\tau)}{\cos \omega_0 \tau} = \frac{R_A(\tau)}{2} \quad (7)$$

Unfortunately, the same calculation with the actual experimental data is not equivalent because the source employed in the experiment did not produce a pure tone, but also contained harmonics as noted in the previous section. Thus,

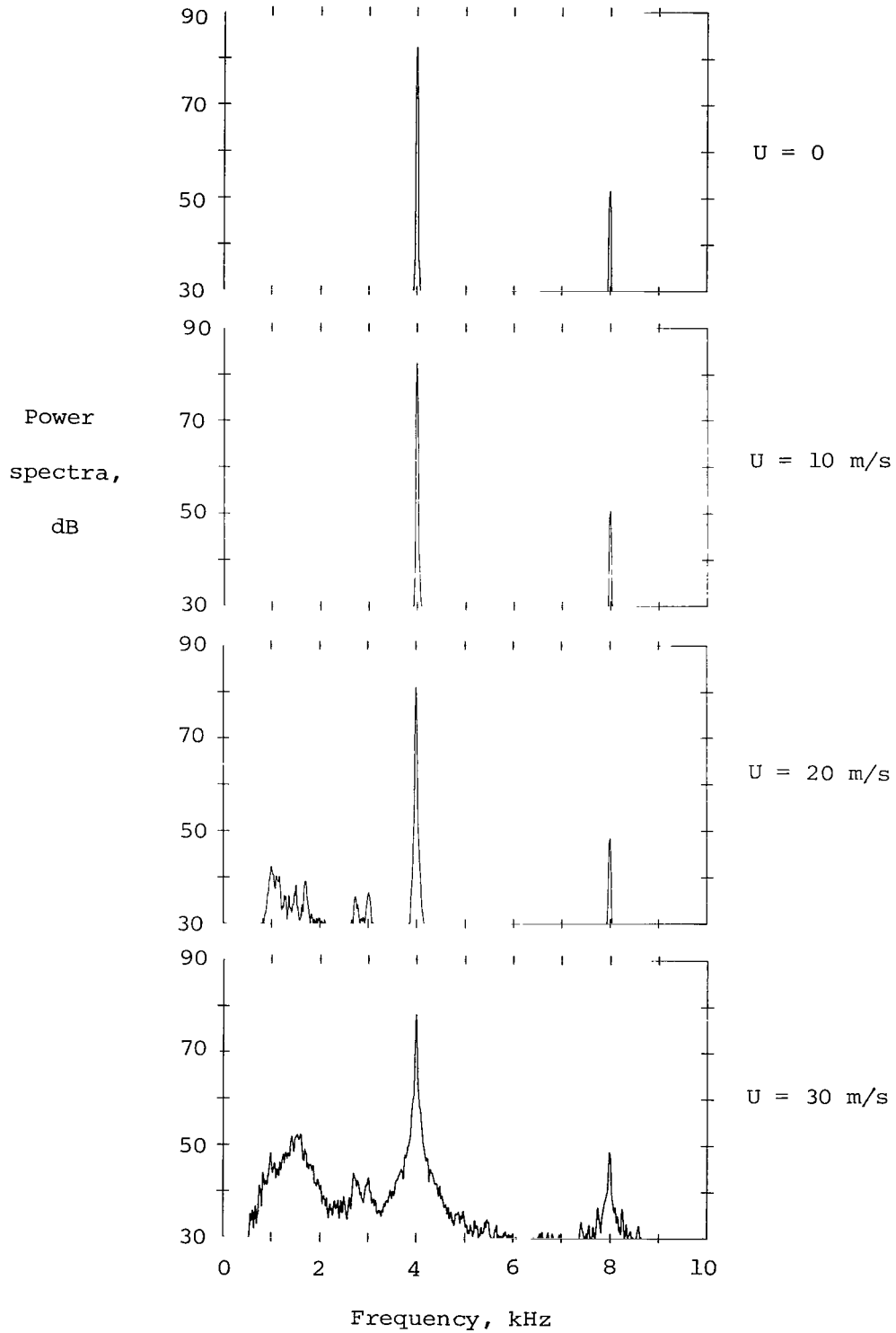


Figure 10.- Power spectra of 30° microphone for several jet velocities. 4-kHz signal.

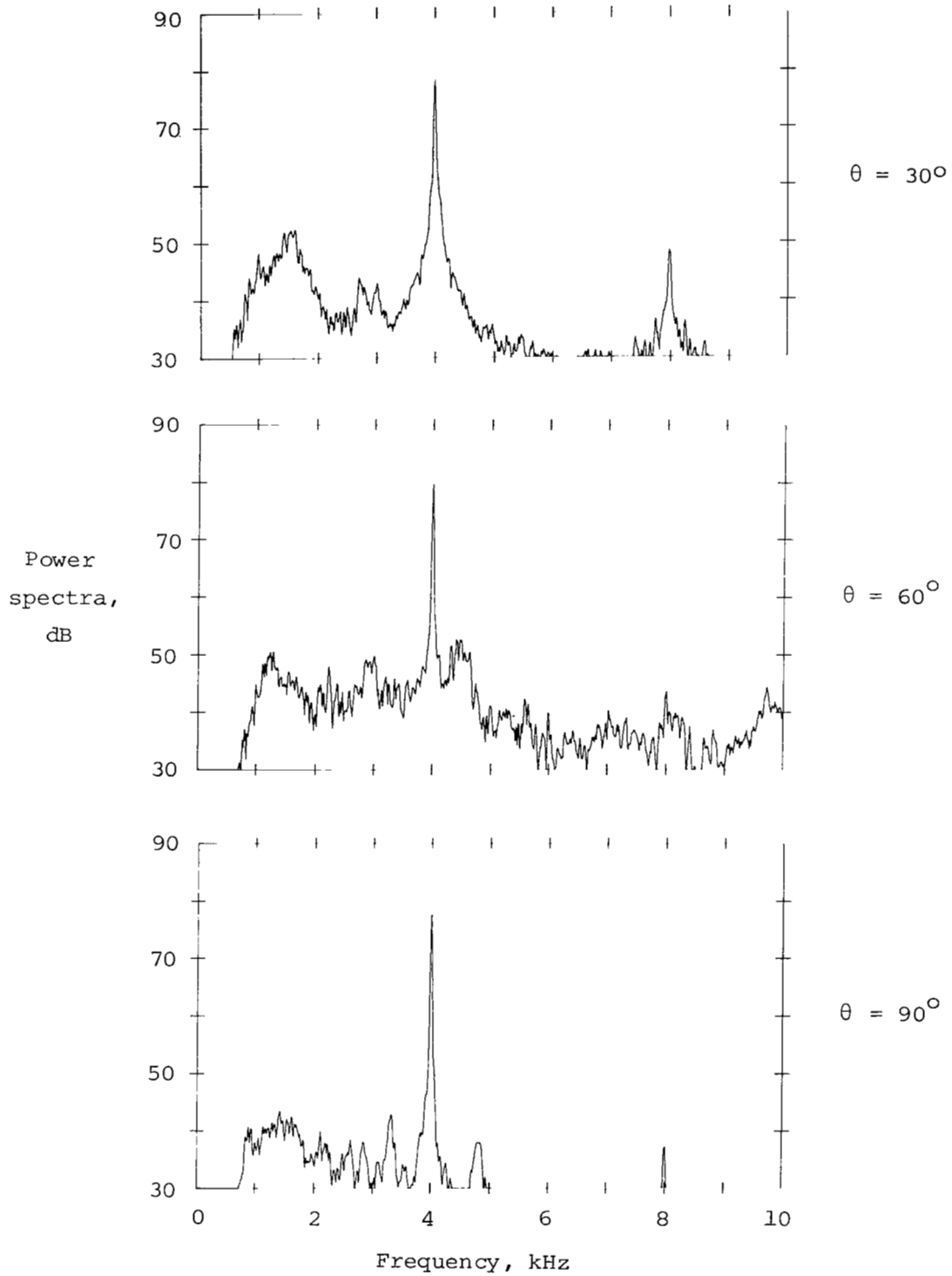


Figure 11.- Power spectra for several far-field positions.
30-m/s jet velocity; 4-kHz signal.

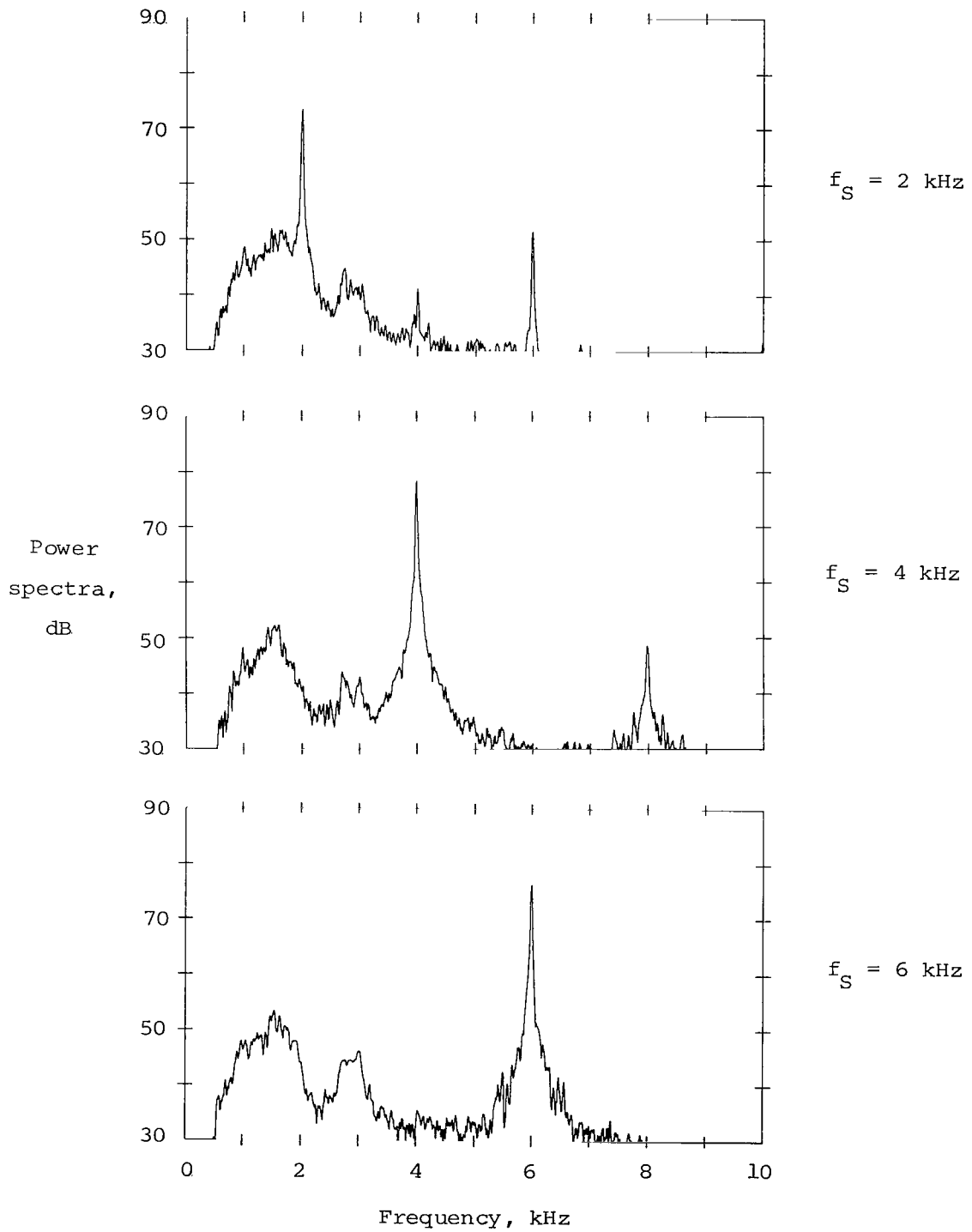


Figure 12.- Power spectra for several source frequencies f_S .
30-m/s jet velocity; 30° microphone.

division of the far-field autocorrelation by the cosine of the fundamental source frequency emphasizes the first harmonic, even though its amplitude is typically at least 20 dB below that of the fundamental.

An equivalent calculation can, however, be accomplished by dividing the acoustic signal autocorrelation by the correlation coefficient of the acoustic source,

$$\rho_S(\tau) = \frac{R_S(\tau)}{R_S(0)}$$

where $R_S(\tau)$ is the autocorrelation of the acoustic signal measured at the source. This operation removes the source characteristics, whatever they might be. The equivalence can be seen from the linearity of equation (7). Thus,

$$\frac{R_{AM}(\tau)}{\rho_S(\tau)} = \frac{R_A(\tau)}{2}$$

in agreement with equation (7).

An example of such a calculation for experimental data at three angles (30°, 60°, and 90°) for a flow speed of 30 m/s and a nominal source frequency of 2 kHz is shown in figure 13. This figure presents the autocorrelation of the far-field acoustic pressure normalized to unit amplitude at $\tau = 0$. The resulting correlation coefficient is divided by the correlation coefficient of the acoustic source. Thus, the plotted curves correspond to estimates of the correlation coefficient, $\rho_A(\tau) = R_A(\tau)/R_A(0)$, of the amplitude-modulation process $A(t)$. These data were obtained by averaging the lagged products from 1 second of data sampled at the rate of 25 000 samples per second to estimate the autocorrelations of both the far-field acoustic pressure and the source signal and then performing the indicated normalizations. Little attention should be paid to the autocorrelation estimates as τ approaches 1 second, since the number of lagged products available for the estimate becomes quite small and thus the variance of the estimate increases. Note that the curves exhibit a virtual spike of unit amplitude at $\tau = 0$ and quite rapidly drop and level out at a reasonably constant lower value as τ increases in agreement with the theory shown in figure 3. This constant value appears to be a function of directivity angle, being approximately 0.94 at 90°, 0.88 at 60°, and near 0.50 at 30°, and can be interpreted as the ratio of the power in the unmodulated acoustic signal to that in the modulated signal, since theory shows that

$$\lim_{\tau \rightarrow \infty} \rho_A(\tau) = \frac{R_A(\infty)}{R_A(0)} = \frac{A_0^2}{A_0^2 + E[\varepsilon^2(t)]}$$

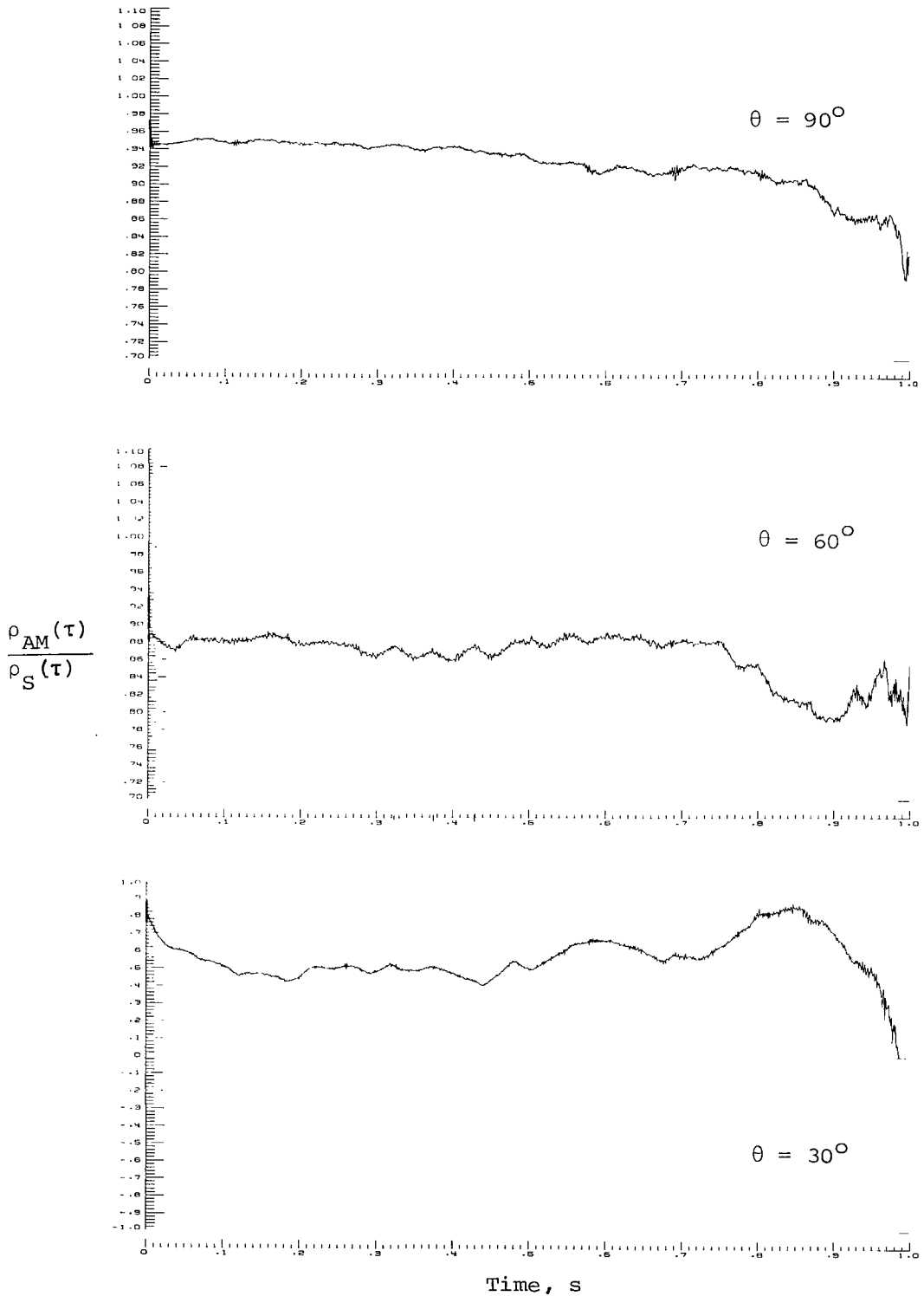


Figure 13.- Normalized autocorrelation of acoustic signal.
 30-m/s jet velocity; 2-kHz signal.

as can be seen from figure 3. Note that this result indicates a substantial amplitude-modulation effect in agreement with the observed time histories shown in figure 9(b). It also implies that if the mean amplitude of the acoustic signal is not changed by the time-varying shear layer, acoustic power is not conserved during the propagation process.

CONCLUSION

This paper has considered the effect of a time-varying shear layer between a harmonic source and an observer on the frequency of the observed sound. Experimental data have shown that the spectral content of the acoustic signal is considerably broadened upon passing through such a shear layer. Theoretical analysis, as well as experimental data, was presented which shows that this spectral broadening is entirely consistent with amplitude modulation of the acoustic signal by the time-varying shear layer. Thus, no actual frequency shift need be hypothesized to explain the spectral data.

Langley Research Center
National Aeronautics and Space Administration
Hampton, VA 23665
April 23, 1981

APPENDIX

COMPARISON OF AMPLITUDE MODULATION WITH FREQUENCY MODULATION

Since the theory of Schlinker and Amiet (ref. 9) implies an actual frequency shift in the acoustic signal, it is of interest to compare the effects of a pure amplitude modulation developed earlier with the effects of a pure frequency modulation. If the time-varying shear layer were to produce an actual frequency modulation of the acoustic signal, the acoustic pressure at the observer could be expressed as

$$p(t) = A_0 \cos [X(t) + \phi] \quad (\text{A1})$$

where $X(t)$, a random process independent of ϕ , represents the modulating effect of the shear layer on the frequency of the acoustic wave. The form assumed in equation (A1) differs slightly from the classical treatment of frequency modulation (see, for example, Papoulis (ref. 13)) in that the random variable ϕ is explicitly considered. This form has advantages in the constraints which must be placed on the process for it to be weakly stationary and is perfectly valid in that the random variable ϕ describes a characteristic completely independent of any action of the time-varying shear layer. Since the effects of the time dependence of the shear layer are small, one can expect that

$$E[X(t)] = \omega_0 t \quad (\text{A2})$$

Further, the expected value of the acoustic signal is again zero, and its auto-correlation is given by

$$R_{FM}(\tau) = E[p(t) p(t+\tau)] = \frac{A_0^2}{2} E \cos [X(t+\tau) - X(t)] \quad (\text{A3})$$

Now, let

$$X(t) = \omega_0 t + w(t) \quad (\text{A4})$$

where $w(t)$ is the frequency-fluctuation process, and from equation (A2), $E[w(t)] = 0$. The joint characteristic function of the random process $w(t)$ is

$$\Phi(\lambda_1, \lambda_2; t_1, t_2) = E \left[e^{i[\lambda_1 w(t_1) + \lambda_2 w(t_2)]} \right] \quad (\text{A5})$$

APPENDIX

Then, the autocorrelation of the frequency-modulated acoustic pressure may be written

$$R_{FM}(\tau) = \frac{A_0^2}{2} \operatorname{Re} \left[e^{i\omega_0\tau} \Phi(-1, 1; t, t+\tau) \right] \quad (A6)$$

where $\operatorname{Re}[\]$ denotes the real part of the complex expression. Thus, it can be seen that a necessary and sufficient condition for the acoustic pressure to be weakly stationary is that the joint characteristic function of the $w(t)$ process depend only on the time difference, i.e.,

$$\Phi(\lambda_1, \lambda_2; t_1, t_1+\tau) = \Phi(\lambda_1, \lambda_2; \tau)$$

Certainly this is true if $w(t)$ itself is second-order stationary. Although such a requirement is not strictly necessary, it is sufficient and will generally be true.

In this case, the final expression for the autocorrelation of the frequency-modulated acoustic wave becomes

$$R_{FM}(\tau) = \frac{A_0^2}{2} \cos \omega_0\tau \operatorname{Re}[\Phi(-1, 1; \tau)] - \frac{A_0^2}{2} \sin \omega_0\tau \operatorname{Im}[\Phi(-1, 1; \tau)] \quad (A7)$$

where $\operatorname{Im}[\]$ indicates the imaginary part of the complex expression.

Now, note that $\Phi(-1, 1; 0) = 1$ because

$$\Phi(-1, 1; \tau) = E \left[e^{i[w(t+\tau) - w(t)]} \right]$$

Also,

$$\lim_{\tau \rightarrow \infty} \Phi(-1, 1; \tau) = |E[e^{i w(t)}]|^2 = \text{Constant} \leq 1$$

because $w(t)$ and $w(t+\tau)$ become independent as $\tau \rightarrow \infty$. Thus, the $\operatorname{Re}[\Phi(-1, 1; \tau)]$ looks very much like the autocorrelation of the amplitude-modulation process $A(t)$ shown in figure 3, and the first term in equation (A7) leads to a power spectral density of the frequency-modulated acoustic pressure very similar to

APPENDIX

that shown in figure 4 for the amplitude-modulated acoustic pressure. The second term in equation (A7) would be expected to be small because if the random process $Z(\tau) = w(t+\tau) - w(t)$ is symmetrically distributed about its mean value $E[Z(\tau)] = 0$,

$$\text{Im}[\Phi(-1,1;\tau)] = E[\sin [w(t+\tau) - w(t)]] \equiv 0$$

This can be seen by considering

$$E[\sin Z] = \int_{-\infty}^{\infty} \sin z f_Z(z) dz \quad (\text{A8})$$

where $f_Z(z)$ is the density function of the random variable $Z(\tau)$. Equation (A8) is the integral of an odd function over even limits. When the second term in equation (A7) is zero, the form of the autocorrelation of the frequency-modulated acoustic wave is exactly the same as that of the amplitude-modulated acoustic wave given by equation (5). Thus, no differentiation of the two is possible on a spectral basis. The only major difference between the two is that the power of the frequency-modulated acoustic pressure is

$$E[p^2(t)] = R_{FM}(0) = \frac{A_0^2}{2}$$

since $\Phi(-1,1;0) = 1$. Thus, frequency modulation is seen to be power preserving in the sense that the power is exactly the same as that of the unmodulated acoustic signal.

REFERENCES

1. Rayleigh, (Lord): The Theory of Sound. First American ed., Volume II, Dover Publ., 1945.
2. Ribner, Herbert S.: Reflection, Transmission and Amplification of Sound by a Moving Medium. J. Acoust. Soc. America, vol. 29, no. 4, Apr. 1957, pp. 435-441.
3. Candel, Sebastian M.; Guedel, Alain; and Julienne, Alain: Radiation, Refraction and Scattering of Acoustic Waves in a Free Shear Flow. AIAA Paper 76-544, July 1976.
4. Howe, M. S.: Multiple Scattering of Sound by Turbulence and Other Inhomogeneities. J. Sound & Vib., vol. 27, no. 4, Apr. 22, 1973, pp. 455-476.
5. Lighthill, James: The Fourth Annual Fairey Lecture: The Propagation of Sound Through Moving Fluids. J. Sound & Vib., vol. 24, no. 4, Oct. 22, 1972, pp. 471-492.
6. Schlinker, Robert H.; and Amiet, Roy K.: Experimental Assessment of Theory for Refraction of Sound by a Shear Layer. NASA CR-145359, 1978.
7. Ahuja, K. K.; Tester, B. J.; and Tanna, H. K.: The Free Jet as a Simulator of Forward Velocity Effects on Jet Noise. NASA CR-3056, 1978.
8. Ozkul, A.; and Yu, J. C.: An Experimental Investigation of Acoustic Radiation From a Source Inside a Large Turbulent Free Jet. J. Acoust. Soc. America, vol. 65, no. 2, Feb. 1979, pp. 336-344.
9. Schlinker, Robert H.; and Amiet, Roy K.: Refraction and Scattering of Sound by a Shear Layer. NASA CR-3371, 1980.
10. Chernov, Lev A. (R. A. Silverman, transl.): Wave Propagation in a Random Medium. Dover Publ., Inc., 1967.
11. Tatarski, V. I. (R. A. Silverman, transl.): Wave Propagation in a Turbulent Medium. Dover Publ., Inc., 1967.
12. Spizzichino, A.: Spectral Broadening of Acoustic and Radio Waves Scattered by Atmospheric Turbulence in the Case of Radar and Solar Experiments. Ann. Geophys., t. 31, nr. 4, Oct.-Nov.-Dec. 1975, pp. 433-445.
13. Papoulis, Athanasios: Probability, Random Variables, and Stochastic Processes. McGraw-Hill Book Co., Inc., c.1965.
14. Maestrello, L.; Bayliss, A.; and Turkel, E.: On the Interaction Between a Sound Pulse With the Shear Layer of an Axisymmetric Jet. J. Sound & Vib., vol. 74, no. 2, Jan. 22, 1981, pp. 281-301.

SYMBOLS

$A(t)$	amplitude of amplitude-modulated acoustic signal
A_0	constant amplitude of unmodulated acoustic signal
D	jet diameter
$f_z(z)$	density function of random variable $Z(\tau)$
l	thickness of shear layer
$p(t)$	acoustic pressure
$R_A(\tau)$	autocorrelation of amplitude-modulation random process
$R_{AM}(\tau)$	autocorrelation of amplitude-modulated acoustic signal
$R_{FM}(\tau)$	autocorrelation of frequency-modulated acoustic signal
$R_{pp}(\tau)$	autocorrelation of unmodulated acoustic signal
$R_S(\tau)$	autocorrelation of source acoustic signal
$R_E(\tau)$	autocorrelation of amplitude-fluctuation random process
$S_A(\omega)$	power spectral density of amplitude-modulation random process
$S_{AM}(\omega)$	power spectral density of amplitude-modulated acoustic signal
$S_p(\omega)$	power spectral density of unmodulated acoustic signal
t	time
U	mean jet velocity
U_c	jet centerline velocity
U_0	axial flow velocity
u'	turbulent intensity in axial direction
$w(t)$	frequency-fluctuation random process
$X(t)$	frequency-modulation random process
$Z(\tau)$	difference random process
z	axial coordinate
$\epsilon(t)$	amplitude-fluctuation

θ directivity angle
 λ_1, λ_2 variables in equation (A5)
 $\rho_A(\tau)$ correlation coefficient of amplitude modulation
 $\rho_{AM}(\tau)$ correlation coefficient of amplitude-modulated signal
 $\rho_S(\tau)$ correlation coefficient of source pressure
 τ time difference
 $\Phi(\lambda_1, \lambda_2; t_1, t_2)$ joint characteristic function of random process $w(t)$
 ϕ random phase angle
 ω circular frequency
 ω_0 nominal circular source frequency
 $E[\]$ mathematical expectation
 $\text{Re}[\]$ real part of expression
 $\text{Im}[\]$ imaginary part of expression

1. Report No. NASA TP-1816		2. Government Accession No.		3. Recipient's Catalog No.	
4. Title and Subtitle STOCHASTIC ANALYSIS OF SPECTRAL BROADENING BY A FREE TURBULENT SHEAR LAYER		5. Report Date May 1981		6. Performing Organization Code 505-32-03-05	
7. Author(s) Jay C. Hardin and John S. Preisser		8. Performing Organization Report No. L-14444		10. Work Unit No.	
9. Performing Organization Name and Address NASA Langley Research Center Hampton, VA 23665		11. Contract or Grant No.		13. Type of Report and Period Covered Technical Paper	
12. Sponsoring Agency Name and Address National Aeronautics and Space Administration Washington, DC 20546		14. Sponsoring Agency Code		15. Supplementary Notes	
16. Abstract <p>This paper considers the effect of a time-varying shear layer between a harmonic acoustic source and an observer on the frequency content of the observed sound. Experimental data have shown that the spectral content of the acoustic signal is considerably broadened upon passing through such a shear layer. Theoretical analysis is presented which shows that such spectral broadening is entirely consistent with amplitude modulation of the acoustic signal by the time-varying shear layer. Thus, no actual frequency shift need be hypothesized to explain the spectral phenomenon. In addition, experimental tests were conducted at 2, 4, and 6 kHz and at free jet flow velocities of 10, 20, and 30 m/s. Analysis of acoustic pressure time histories obtained from these tests confirms the above conclusion, at least for the low Mach numbers considered.</p>					
17. Key Words (Suggested by Author(s)) Spectral broadening Sound propagation Shear layer			18. Distribution Statement Unclassified - Unlimited		
19. Security Classif. (of this report) Unclassified			20. Security Classif. (of this page) Unclassified		21. No. of Pages 24
					22. Price A02
Subject Category 71					

National Aeronautics and
Space Administration

THIRD-CLASS BULK RATE

Postage and Fees Paid
National Aeronautics and
Space Administration
NASA-451



Washington, D.C.
20546

Official Business

Penalty for Private Use, \$300

4 1 1U,H, 052281 S00903DS
DEPT OF THE AIR FORCE
AF WEAPONS LABORATORY
ATTN: TECHNICAL LIBRARY (SUL)
KIRTLAND AFB NM 87117

NASA

POSTMASTER: If Undeliverable (Section 158
Postal Manual) Do Not Return
